J. theor. Biol. (1996) **181,** 179–196

Optimal Sets of Color Receptors and Color Opponent Systems for Coding of Natural Objects in Insect Vision

LARS CHITTKA†

Institut für Neurobiologie, FU Berlin Königin-Luise-Str. 28-30, 14195 *Berlin, Germany and the Department of Ecology and Evolution, State University of New York, Stony Brook, NY* 11794-5245, *U.S.A.*

(*Received on* 31 *August* 1995, *Accepted in revised form on* 12 *April* 1996)

Model calculations are used to find an optimal color vision system for the coding of natural objects. The criteria to assess the quality of color vision are (a) discriminability between all colors of a given set; (b) discriminability between nearest neighbors (only the most similar colors of a set); and (c) detectability (color difference between target and background). The colored objects investigated are several sets of flower colors, one set of green foliage colors, and one set of fruit colors. A large variety of hypothetical color vision systems was generated by varying both the wavelength positions of photoreceptors and the weights of color opponent processes used to evaluate the receptor inputs. It is shown that the set of spectral receptor types in flower visiting bees (λmax = 340, 430 and 540 nm) is close to optimal for the discrimination of several sets of sympatric and simultaneously blooming flower colors, as well as for discrimination of green foliage, but not for fruit coloration. For two sets of objects, the illuminant was varied, which changed the results only marginally. Detectability of flowers against background is likewise optimal. The optimal wavelength positions of photoreceptors are largely independent of the particular color opponent mechanisms used to evaluate the photoreceptor signals. Optimal color opponent systems are all those which comprise two opponent processes with weighting factors differing strongly from one another. The evolutionary implications of these findings are discussed against the background of a recent phylogenetic study which showed that wavelength tuning of insect photoreceptors likely predated the evolution of flower color.

Introduction

Different animal species often see the world in substantially different colors, and it is likely that some of these differences are adaptive for a given colored environment (Lythgoe & Partridge, 1989, 1991; Chittka & Menzel, 1992; Endler, 1992; Nagle & Osorio, 1993). It is often difficult to pin-point which components of the environment might drive the evolution of color vision, but in flower-visiting Hymenoptera, the evolutionarily significant objects are comparatively easily determined. Plants contain the major nutrition—pollen and nectar—for these insects, and they advertise these rewards by means of species-specific signals, the flowers (Feinsinger, 1987; Kevan & Baker, 1983; Menzel & Shmida, 1993; Chittka *et al.*, 1993; Waser *et al.*, 1996) The swift detection of such signals from their background is thus of vital interest. Furthermore, bees have to make economic choices within a multitude of different flower species with different colors and information contents about rewards and their accessibility (Giurfa *et al.*, 1995). Selection will thus favor flower-visitors that are able to learn the features of any plant species and distinguish it from others in a community. Accumulating confusions of floral signals may result in a decrease in foraging efficiency, and thus in a reduced fitness of the pollinator. Consequently, the ability to discriminate and detect floral colors is particularly important for anthophilous Hymenoptera.

Indeed, it was shown that the sets of spectral receptor types in Apidae (λmax = 340, 430 and

† Present address: Ecology & Evolution, State University of New York, Stony Brook, NY 11794-5245, U.S.A. Email: chittka@life.bio.sunysb.edu

540 nm) are very close to optimal for distinguishing between floral hues of one particular set of 180 Israeli flower colors (Chittka & Menzel, 1992). This conclusion must be further substantiated. First, it is conceivable that this result is obtained with only one particular set of flower colors, but fails in several others. Second, it is also important to distinguish flowers from the background, not only from signals of other species in the same environment. Third, the photoreceptors do not solely define the metrics of an animal's percept of color. It is also important to consider the mechanisms of color coding with respect to the ecological demands of a species. Here I describe novel model calculations to find optimal solutions for all of these tasks. Finally, a recent phylogenetic analysis revealed that bee color vision may be older than the emergence of angiosperm flowers (Chittka, 1996). Thus, I will examine the possibility that wavelength positions of insect UV-, blue and green receptors are adapted to code for objects in a pre-angiosperm world, such as green leaves.

Methods

SPECTRAL MEASUREMENTS

The reflectance spectra of flowers were measured by means of a photodiode-array-spectrophotometer (SR01, Fa. Gröbel; Ettlingen; Germany). The reader is referred to Chittka & Menzel (1992) for preparation of flowers and details of the measurement procedure. Several samples of natural colors are evaluated here. These include six sets of flower colors from species which are all blooming sympatrically and simultaneously, including a German dry grassland meadow, a Brazilian Cerrado, a Norwegian and one Austrian Alpine valley, and a German continental forest [Chittka (1993), all of these were measured in the summer] the Hatzeva desert in Israel in spring (Menzel & Shmida, 1993). Further sets of natural stimuli are a collection of 230 leaf reflectance spectra (Chittka *et al*., 1994) and a set of fruits from 35 different species purchased in a Berlin department store (Chittka, unpublished).

DETERMINATION OF COLOR LOCI IN THE COLOR HEXAGON

Spectral sensitivity of a photoreceptor with a given λmax is calculated according to Stavenga *et al*. (1993). The relative amount of light absorbed by each photoreceptor color type is:

$$P = R\int_{300}^{700} I_S(\lambda)S(\lambda)D(\lambda)\mathrm{d}\lambda \qquad (1)$$

where $I_S(\lambda)$ is the spectral reflectance function of the stimulus in question; $S(\lambda)$ is the spectral sensitivity function of the receptor in question and $D(\lambda)$ is the illuminating daylight spectrum. Normfunction D65 (Wyszecki & Stiles, 1982) is employed wherever open habitats are concerned (Fig. 1). For two sets of stimuli (the German continental forest habitat, and the set of green leaves) the model calculations were also performed using a forest shade spectrum [courtesy of Dr. John Endler, see Endler (1993)]. This measurement extends only down to 350 nm; however, all insects so far tested have UV receptors which are maximally sensitive at about this value (Chittka, 1996), and whose sensitivity extends considerably below 350 nm. For this reason, the spectrum was extrapolated to 300 nm in a gentle slope, following leaf reflectance measurements which covered the entire range from 300–700 nm (Chittka *et al*., 1994). The resulting spectrum is shown in Fig. 1. The sensitivity factor R in eqn. (1) is determined by the equation

$$R = 1/\int_{300}^{700} I_B(\lambda)S(\lambda)D(\lambda)\mathrm{d}\lambda \qquad (2)$$

$I_B(\lambda)$ is the spectral reflection function of the background to which the receptors are adapted. With this model, it is assumed that the photoreceptors display half their maximal response when stimulated by the light reflected from the adaptation background. While this assumption may fail when strongly chromatic backgrounds are used (Dittrich, 1995) it predicts the relative sensitivities of the photoreceptors well so long as the background has a roughly equiproportionate reflectance over the visual spec-

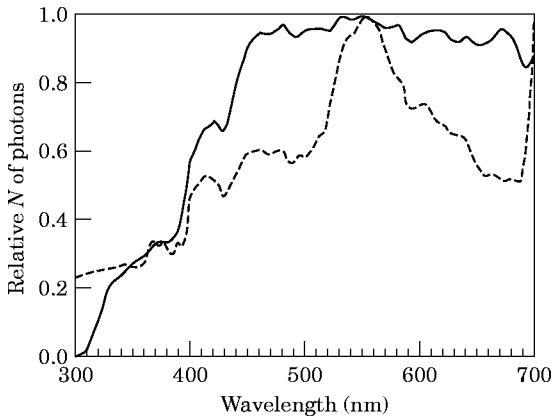

FIG. 1. Illumination functions employed in the present study, normalized to a maximum of unity. The continuous line denotes the normfunction D65 (Wyszecki & Stiles, 1982); the dashed line is a function measured in forest shade (courtesy of Dr John Endler).

trum (Brandt *et al*., 1993), as is the case for most natural background materials in the visual range of trichromatic insects (Daumer, 1958; Lythgoe, 1979; Endler, 1992; Chittka *et al*., 1994). Only for receptors with $\lambda\max < 350$ nm, eqn (2) will produce unrealistically high sensitivities relative to the other two receptor types (Chittka & Menzel, 1992). Helversen (1972) found that the honeybee's UV receptor is not more than 16.5 times more sensitive than the green receptors under illumination conditions practically without UV. Hence it is assumed that receptors with $\lambda\max < 350$ nm are maximally 16.5 times more sensitive than a green receptor at 550 nm. For further detail, see Chittka & Menzel (1992).

The quantum catch in the photoreceptors P [eqn (1)] is the input to the photoreceptors, not the input to the insect brain. On a neural level, the brain performs "calculations" with graded potentials generated by receptor cells. These signals are not linearly related to the logarithm of the quantum flux that forms the input to the receptor (Naka & Rushton, 1966). When the maximum excitation $E_{\max}$ of the photoreceptors is set to one, the nonlinear phototransduction process is well described by

$$E = P/(P + 1) \tag{3}$$

where P is the stimulus strength [eqn (1)], in units such that for $P = 1$, $E = 0.5$ [i.e. half the maximum potential; Naka & Rushton (1966)]. With the transduction process modeled in this fashion, very precise predictions of both electrophysiological (Lipetz, 1971; Laughlin, 1989) and behavioral (Valberg, 1986; Backhaus, 1992) data are possible, even when stimulus intensity is varied over several log units. The three excitation values in the bee's UV, blue and green receptors can be depicted in a three-dimensional receptor excitation space [Fig. 2(c)] or in the color hexagon [Fig. 2(d)]. The geometry of the color hexagon has been described elsewhere in detail (Chittka, 1992). Since, however, this color space forms a conceptual axis in the present paper, linking graphically the photoreceptor signals and various systems of opponent coding, I will outline its basic philosophy here. The color hexagon may be understood as a two-dimensional projection of the three-dimensional receptor space [Fig. 2(d)]. This projection is legitimate because Hymenoptera of several genera do not evaluate the brightness component of color signals at the feeding site (Chittka *et al*., 1992). With the three receptor excitation values now plotted at angles of 120° [Fig. 2(d, e)], the x and y coordinates in the color plane are given by:

$$x = \cos 30^\circ * (\mathbf{E_L} - \mathbf{E_S})$$

$$\Leftrightarrow \qquad x = \sqrt{3}/2 * (\mathbf{E_L} - \mathbf{E_S}) \tag{4}$$

and

$$y = \mathbf{E_M} - 0.5 * (\mathbf{E_L} + \mathbf{E_S}) \tag{5}$$

where $\mathbf{E_S}$, $\mathbf{E_M}$ and $\mathbf{E_L}$ are the inputs from the short, middle and long wave receptors [according to eqn (3)]. Since the wavelength positions of receptors will be varied in the model calculations to be described below, we will use these more general indices rather than $\mathbf{E_U}$, $\mathbf{E_B}$ and $\mathbf{E_G}$.

THE COLOR HEXAGON AS A GENERALIZED COLOR OPPONENT SPACE

The excitation A of a color opponent mechanism is defined by

$$A = a\mathbf{E_S} + b\mathbf{E_M} + c\mathbf{E_L}. \tag{6}$$

a, b, c are the weighting factors. We define that $a + b + c = 0$; this is necessary on theoretical grounds for an intensity-independent perception of white (Chittka *et al*., 1992; Abramov & Gordon, 1994). Moreover, this condition has been explicitly shown to hold in the honeybee (Backhaus, 1991). Thus,

$$A = a\mathbf{E_S} + b\mathbf{E_M} - (a + b)\mathbf{E_L}. \tag{7}$$

From (2) and (3), it follows that:

$$\mathbf{E_S} = \mathbf{E_L} - 2/\sqrt{3} * x$$

and

$$\mathbf{E_M} = y + \mathbf{E_L} - x/\sqrt{3}$$

Thus, replacing $\mathbf{E_S}$ and $\mathbf{E_M}$ in eqn (7), we obtain:

$$A = a * (\mathbf{E_L} - 2/\sqrt{3} * x) + b * (y + \mathbf{E_L} - x/\sqrt{3})(a + b) * \mathbf{E_L}$$

$$\Leftrightarrow \qquad A = -x/\sqrt{3} * (2a + b) + b * y. \tag{8}$$

Thus, the excitation value for any opponent mechanism with known weighting factors a and b can be derived from the hexagon coordinates x and y, provided that $a + b + c = 0$. To read the excitation value for such an opponent mechanism directly from the hexagon coordinates determined by a given colored stimulus with receptor excitation values $\mathbf{E_S}$, $\mathbf{E_M}$ and $\mathbf{E_L}$, it is useful to draw a color opponent axis through the color plane. For this purpose, we must find the linear equation $y = mx + n$ that corresponds to an opponent axis with known weighting factors.

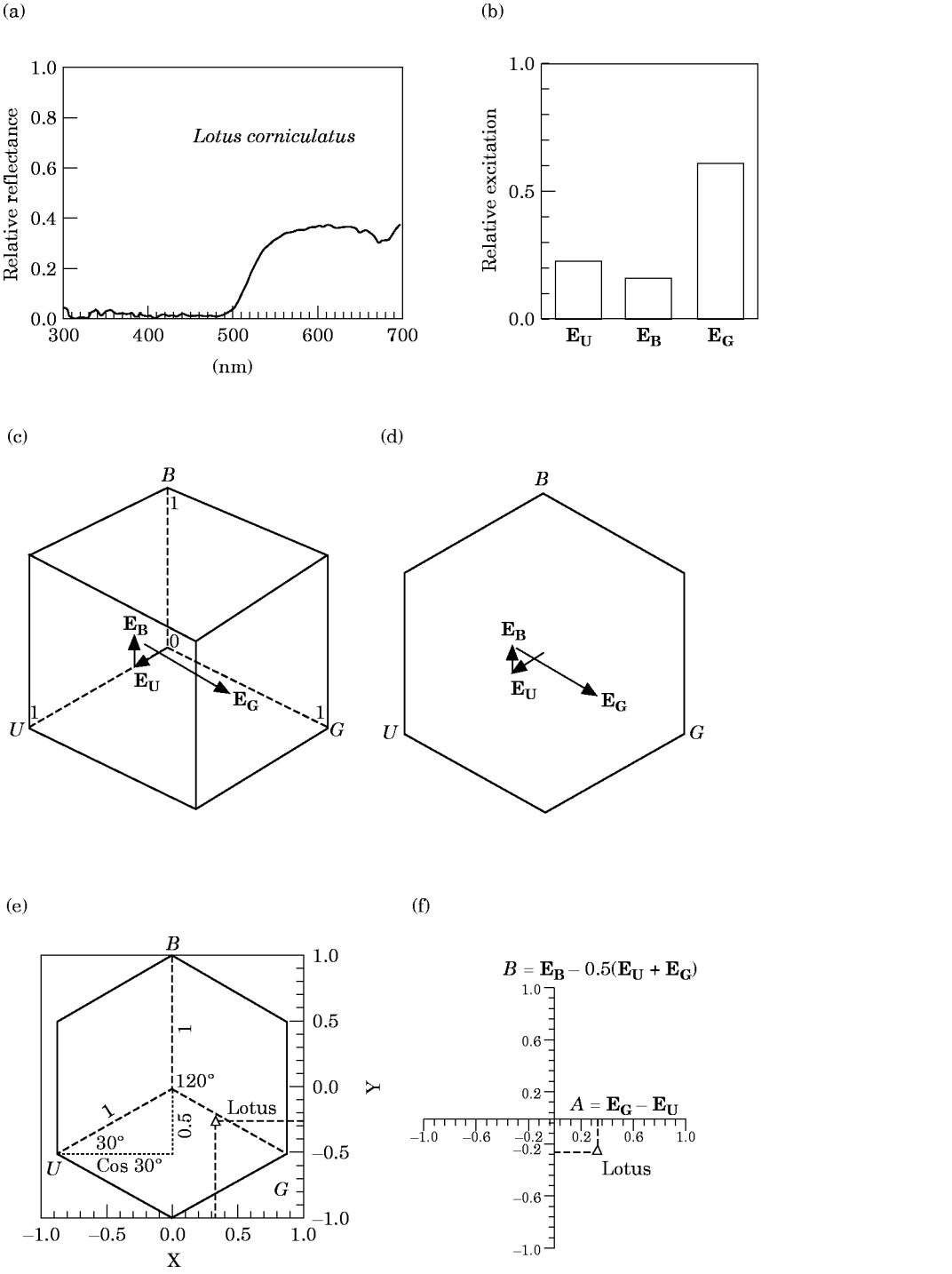

FIG. 2. From object spectral reflectance to a locus in the color hexagon, and further to a point in an opponent color space. (a) shows the reflection function of *Lotus corniculatus*, a flower which appears yellow to humans and green to bees. (b) Receptor excitations $\mathbf{E}_U$, $\mathbf{E}_B$ and $\mathbf{E}_G$ are calculated according to eqns (1–3). Excitation values are given relative to the maximum possible excitation in each receptor type. **c)** $\mathbf{E}_U$, $\mathbf{E}_B$ and $\mathbf{E}_G$ plotted as vectors in a three-dimensional receptor excitation space. Dashed lines denote the back side of the cube. The vectors originate in the point marked "0". The brightness dimension corresponds to an axis linking the point marked "0" and the upper frontal corner. The tip of the $\mathbf{E}_G$-vector indicates the point generated by *Lotus* in color space. (d) The color hexagon is a two-dimensional projection of the three dimensional color space. Consider the cube in (c) with the brightness dimension removed—the projected plane of the cube is a hexagon. Vectors $\mathbf{E}_U$, $\mathbf{E}_B$ and $\mathbf{E}_G$ then come to lie at equal angles of 120°. (e) These three vectors can be easily converted into orthogonal X/Y coordinates trigonometrically. In the Y direction, the weight of $\mathbf{E}_B$ is $+1$, whereas those of $\mathbf{E}_U$ and $\mathbf{E}_G$ are -0.5. On the X axis, the weights for $\mathbf{E}_U$ and $\mathbf{E}_G$ are $-\cos 30°$ and $+\cos 30°$, respectively. The triangle marks the color point occupied by *Lotus* as determined by the three vectors $\mathbf{E}_U$, $\mathbf{E}_B$ and $\mathbf{E}_G$ in Fig. 1(d). (f) Any two-dimensional color opponent space defined by two of the three eqns (12–14) is a linear transformation of the color hexagon. For simplicity, the example given is a plane whose dimensions (blue vs. UV-green, and UV vs. green) correspond directly to the X/Y coordinates in the color hexagon. In general, the color opponent space is constructed using two scales corresponding to two different formulae of the kind $A = a\mathbf{E}_U + b\mathbf{E}_B + c\mathbf{E}_G$ (where $a + b + c = 0$) and plotting these scales orthogonally.

For simplicity reasons, I will start out by constructing an axis which runs through the origin (the center of the hexagon), i.e. $n = 0$. In this case, the slope m is determined by $m = y/x$. Replacing the receptor excitations $\mathbf{E}_S$, $\mathbf{E}_M$ and $\mathbf{E}_L$ in the equation by their weights a, b and c, we obtain:

$$m = \frac{b - 0.5*(a + c)}{\sqrt{3}/2*(c - a)}$$
$$\Leftrightarrow \quad m = \frac{\sqrt{3}b}{-2a - b},$$

since $a + b + c = 0$. Thus, the linear equation for an opponent axis with known weighting factors a and b is:

$$y = \frac{\sqrt{3}b \times x}{-2a - b} \tag{9}$$

when the axis runs through the origin. For some purposes, it may be convenient to displace the axis parallely, so that it retains the same orientation, but no longer runs through the center of the hexagon (Chittka *et al*., 1992). For this reason, the y-intercept n in the linear equation $y = mx + n$ must be determined. If we know the coordinates x_1 and y_1 which we want to be intercepted by the opponent axis, n is determined by $n = y_1 - mx_1$. Thus,

$$n = y_1 - \frac{\sqrt{3}b}{-2a - b}\, x_1. \tag{10}$$

Adding the y intercept [according to eqn (10)] to eqn (9), the entire linear equation for a color opponent axis with weighting factors a and b, which runs through a point x_1, y_1, is as follows

$$y = \frac{\sqrt{3}b}{-2a - b} \times x + y_1 - \frac{\sqrt{} \times 3}{-2a - b}\, x_1$$
$$\Leftrightarrow \qquad y = \sqrt{3}b/(-2a - b)(x - x_1) + y_1 \tag{11}$$

In some of the model calculations to be described below, different pairs of color opponent mechanisms will be generated, to see how opponent coding affects color discriminability. There are three possible color opponent mechanisms that follow eqn (6). These are:

S vs. *ML*

$$A = aE_S + bE_M + cE_L \text{ where } a = 1 \tag{12}$$

M vs. *SL*

$$B = aE_S + bE_M + cE_L \text{ where } b = 1 \tag{13}$$

L vs. *SM*

$$C = aE_S + bE_M + cE_L \text{ where } c = 1 \tag{14}$$

and $a + b + c = 0$ in all these three (see above).

One of the variable factors in each of these equations will be varied from 0 to 1 in steps of 0.25, so that five versions of each color opponent mechanism (12–14) are generated. Figure 3 shows how the five sets of weighting factors for the *S* vs. *ML* mechanism relate to color opponent axes in the hexagon. I have chosen the convention that all axes assigned to the mechanisms (12–14) should run through one of the corners of the color hexagon. For example, for the *S* vs. *ML* mechanism (Fig. 3), all axes intercept the lower left (labeled *U*) corner of the

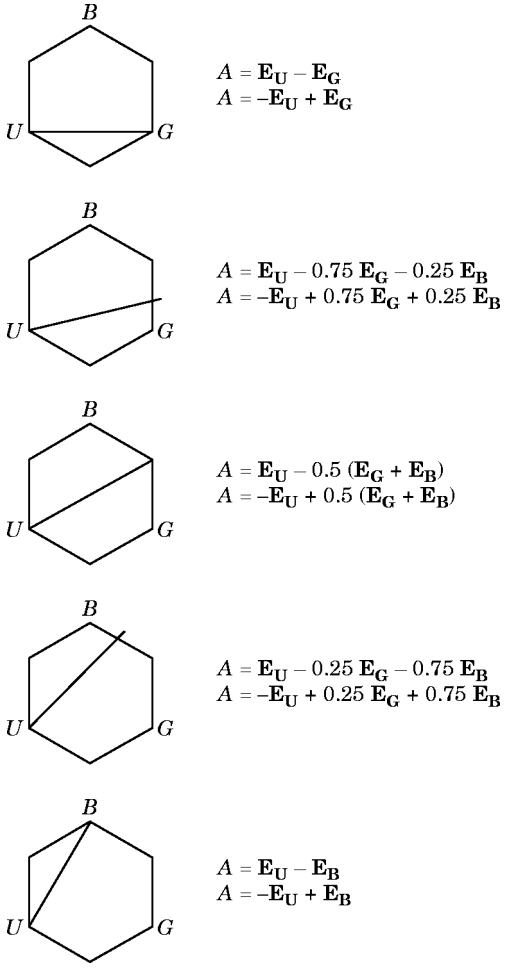

FIG. 3. Relationship of color opponent axes in the hexagon and weighting factors of five color opponent mechanisms according to eqns (11) and (12). Mechanisms with mirror image inputs correspond to the same axis (Chittka *et al*., 1992). All axes intercept the "U" corner of the hexagon, to make explicit the fact that in all opponent processes illustrated here, the weighting factor for $\mathbf{E}_U$ is 1. The weights of $\mathbf{E}_B$ and $\mathbf{E}_G$ are varied, and their relative strengths can be estimated by evaluating the distance at which the axes intercept the straight line between the *B* and *G* corners of the hexagon. For example, when the weight for $\mathbf{E}_B$ is 1 and that for $\mathbf{E}_G$ is 0, as in the lower hexagon symbol, the axis will run through the *B* corner. When both weights are equal (0.5, as in the central hexagon symbol), the axis will cut the straight line between the *B* and *G* corners into two equal portions.

hexagon [i.e. $x_1 = -\sqrt{3}/2$ and $y_1 = -0.5$ in eqn (11)]. For the *M* vs. *SL* opponent mechanism, all axes run through the upper corner (*B*) of the hexagon, and for the *L* vs. *SM* mechanism, all axes intercept the lower right corner (*G*). On three levels, this convention makes explicit which weighting factors are used for the opponent processes, and how they are varied: (a) If one of the weighting factors *a*, *b* or *c* in the equation $A = a\mathbf{E}_S + b\mathbf{E}_M + c\mathbf{E}_L$ is 1 or -1, the axis will run through one of the corners of the hexagon which correspond to the endpoints of the $\mathbf{E}_S$, $\mathbf{E}_M$ or $\mathbf{E}_L$ vectors. When $a = 1$, this will be the lower left corner (the endpoint of the $\mathbf{E}_S$ vector), and so forth (Fig. 3). If two weighting factors in a single color opponent process are 1 and -1, two corners of the hexagon will be connected. (b) When one weighting factor is constant, and the other two varied, all axes corresponding to the set of opponent processes so generated will run through the same corner of the hexagon. This corner is determined as in (a); (c) the relative strength of the two *varied* weighting factors can be easily estimated. In Fig. 3, factors *b* and *c* are varied from 0 to 1 (or 1 to 0, respectively), these weights are expressed in terms of where the axis intersects the straight line between the endpoints of the $\mathbf{E}_M$ or $\mathbf{E}_L$ vectors. For example, if both *b* and *c* are 0.5, the corresponding axes will intersect this line in the middle.

The difference between two color opponent mechanisms can be estimated by measuring the angle between the two hexagon axes corresponding to these mechanisms (Chittka, 1992). If this angle is small, the two mechanisms will render similar values for a given set of stimuli. In other words, the information provided by two color opponent mechanisms is highly interdependent, and thus redundant, when angles between axes are minimal. Thus, it is predicted that natural color coding systems should use opponent mechanisms whose assigned axes differ significantly with respect to their orientation in the hexagon. Indeed, when one looks at color opponent systems in several species of trichromatic Hymenoptera, one finds that the axes corresponding to their individual color opponent mechanisms are usually large (Chittka *et al*., 1992).

Model Calculations and Results

OPTIMAL COLOR RECEPTORS FOR DETECTION OF FLOWERS AGAINST GREEN FOLIAGE

If the wavelength position of a photoreceptor is altered, the two-dimensional distribution of color loci in the color space changes (Fig. 4). Correspondingly, the perceptual distances between colors change. Detectability is optimal when the color distances of all floral color loci to their background are maximized. To test which spectral photoreceptor set is optimal for this purpose, I used a background reflectance curve averaged from several green leaves (Chittka *et al*., 1994). I then proceeded to vary the wavelength positions of the spectral receptors, to see how this variation effects color distances between 180 Israeli flower colors and the green foliage locus in color space. Since the three receptor signals are assumed to be adapted to the background reflectance, the green foliage locus comes to lie in the center of color space.

In each of three variations, one receptor was varied in 10 nm steps, and the two others were held constant at the wavelength positions where they occur in Hymenoptera. For every such combination of photoreceptors all differences between flower colors and the green foliage point in the hexagon are calculated and summed up (Fig. 5). The resulting optima for these sums of perceptual differences at 330, 430 and 550 nm agree very well with the photoreceptor wavelength positions as found in the eyes of Hymenoptera (Fig. 5, inset). The calculated optimal photoreceptors deviate from the most frequent "real" receptors by maximally 10 nm.

OPTIMAL COLOR RECEPTORS FOR DISCRIMINATION OF SIMILAR FLOWER COLORS

The trichromatic receptor set of most bee species is also well adapted for discrimination between flower colors of different species, when the quality of the system is assessed by the sum of all color differences between all objects in question (Chittka & Menzel, 1992). Alternatively, one might argue that discriminability of objects with large color differences need not necessarily be maximized. Signals that are located far apart in a color space determined by one set of sensory inputs will, with some probability, also be far apart in a color space whose sensory inputs have been altered. Thus, I also calculated an optimal photoreceptor set by evaluating only the nearest neighbor color differences in color space.

To this end, I determined the three closest color loci of the flowers of different species from each floral color locus. All of these values were summed for each set of spectral receptor types. As in the model calculations described above, the resulting optima for the *S*-, *M*- and *L*-receptors correspond closely to those found in trichromatic bees and wasps, and so their color vision is also well suited to distinguish flower colors of high similarity, i.e. such signals which are most likely to be confused (Fig. 6, lines with short dashes).

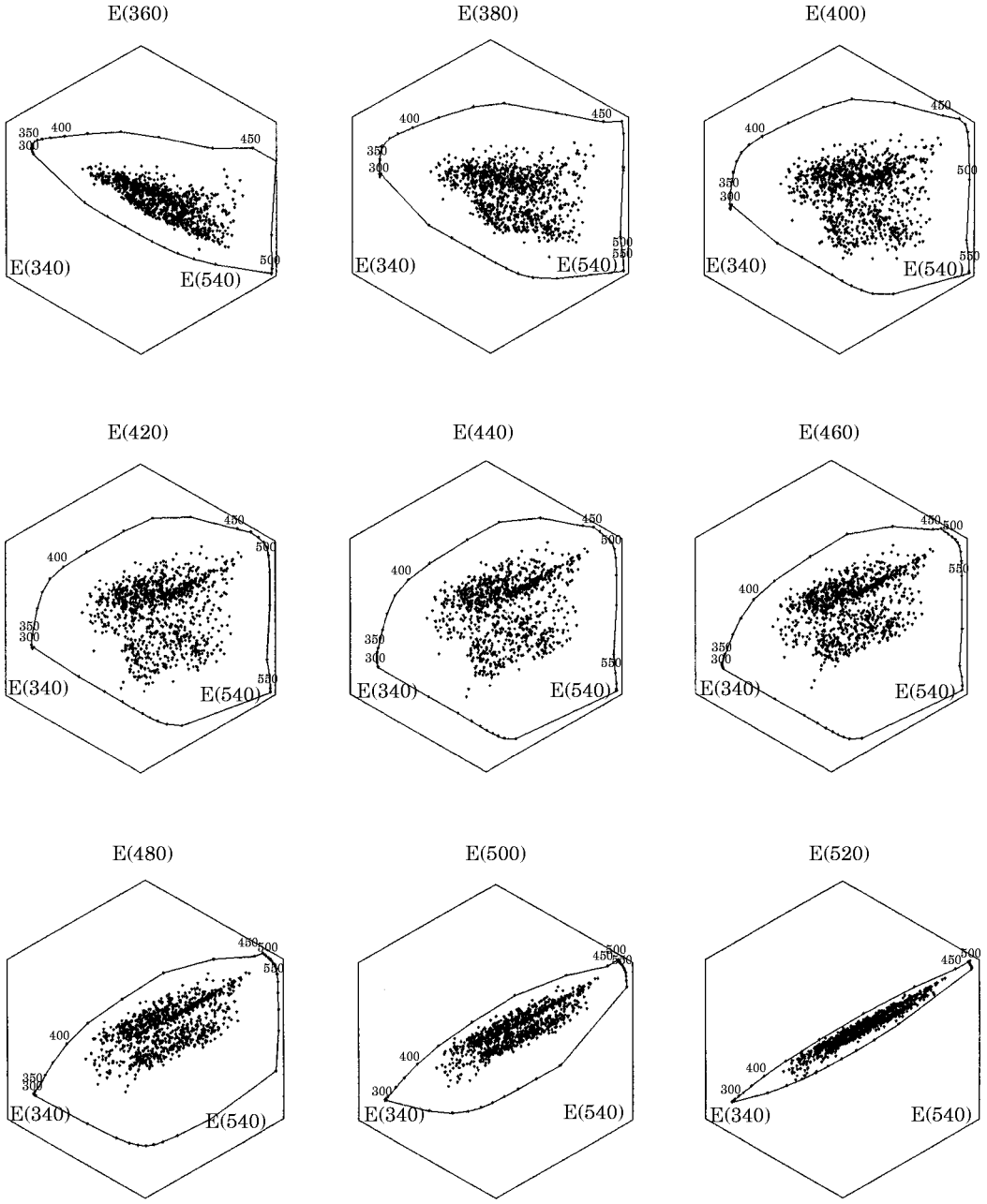

FIG. 4. Distribution of 1063 flower color loci in color space, depending on the wavelength positions of receptors. The short wave receptor is fixed at λmax = 340 nm, and the long wave receptor at λmax = 540 nm. The middle wave (M) receptor is shifted from 360 to 520 nm in 20 nm steps. The irregular polygon inside the hexagon is the spectrum locus, which marks the periphery of the color space outside which no loci can be reached. It connects the color points generated by monochromatic lights from 300 to 550 nm, in 10 nm steps. Since the locus of a single wavelength changes with intensity (Backhaus, 1992; Chittka, 1992), intensity is adjusted in each spectral light to generate a maximal distance between color locus and uncolored point. The S and L ends of the spectrum locus are connected by mixing 300 and 550 nm in nine mixture ratios. Floral reflectance data from Chittka *et al*. (1994).

Is this result a consequence of fixing two receptors and shifting only the third one? Would a shift of the entire receptor set yield unchanged information for different wavelength positions, or is the tuning of the entire set also critical? To answer this question, a simulation was performed in which all three receptors were shifted in concert, keeping the wavelength spacing between receptors constant. The difference between the λ_{max} of the S receptor and that of the M receptor is commonly $\sim$90 nm, whereas the difference between the S and L receptors is most often $\sim$200 nm (Peitsch *et al*., 1992). These differences were used in the simulation. The S-receptor was shifted from 300 to 450 nm in 10 nm steps, and the other two assumed

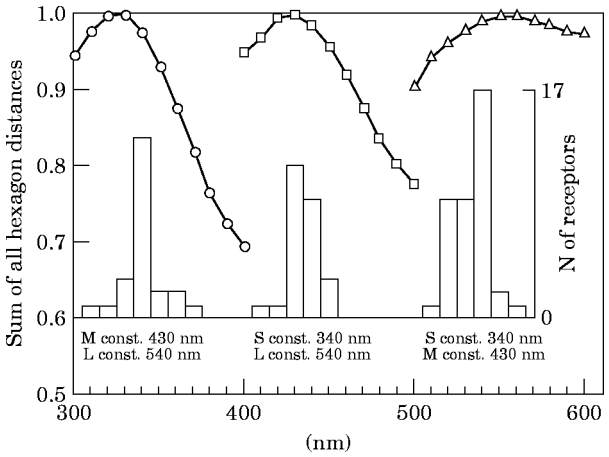

FIG. 5. Optimal wavelength positions of photoreceptors for detection of floral colors against green foliage. In each of three variations, two receptors were clamped at the wavelength positions where they most frequently occur in Hymenoptera (λ_{max} = 340, 430, 540 nm, see inset), and the third was shifted in 10 nm steps from 300 to 400 nm, from 400 to 500 nm or from 500 to 600 nm. For each combination of spectral receptor types, distances between all floral color loci and the green foliage background were determined. All of these distance values were summed up, and plotted in the diagram so that the maximum of each curve equals one. The inset shows the absolute number of photoreceptors recorded at every given λ_{max} for 40 different species of Hymenoptera (Peitsch *et al*., 1992).

positions with constant distances to the *S* receptor. Under these conditions, the optimal set (λ_{max} = 330, 420, 530 nm) is only 10 nm away from the most common "real" set (λ_{max} = 340, 430, 540 nm; Fig. 6).

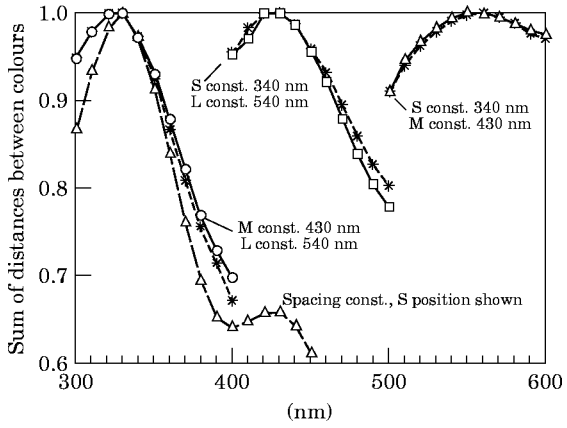

FIG. 6. Optimal sets of three spectral receptor types for the discrimination of flower colors. The spread of 180 flower colors was measured depending on which set of spectral photoreceptors was used. For every such set all the hexagon distances between every pair of color signals were determined. The sums of all these distances are plotted for each receptor set tested (result taken from Chittka & Menzel, 1992). The curves with short dashes denote the sums of nearest neighbor color distances only. Both optimality criteria yield almost indistinguishable results. Sums of color distances are also shown for a simulation in which the spacing between photoreceptors was kept constant at values most frequently found in Hymenoptera, i.e. $\lambda_{max}(M) - \lambda_{max}(S) = 90$ nm, and $\lambda_{max}(L) - \lambda_{max}(M) = 110$ nm (triangles and long dashes). The abscissa denotes the *S* receptor position for this simulation.

Thus, not only the spacing but also the absolute wavelength tuning of the photoreceptor set is critical for discrimination of natural objects. The simulation generates a secondary peak at the following positions: λ_{max} = 430, 520, 630 nm, which is interesting because *S* and *M* receptor positions close to these values are common in many mammals (Jacobs, 1993).

OPTIMAL COLOR RECEPTORS FOR DISCRIMINATION OF SYMPATRIC FLOWERS

So far I have tested discriminability of objects that the individual insect might not necessarily encounter simultaneously, or even during its lifetime. The above considerations refer to the general concept that an animal should be able to distinguish as many colors of biologically relevant objects as precisely as possible. From an ecological point of view, it is likewise interesting to ask if pollinator color vision is optimally suited to discern floral colors that occur in close spatial relationship. For this purpose I selected six sets of sympatric plant species which bloom simultaneously. The distinction of these flowers is a task encountered by any insect that forages in these plant arrays; successful distinction should be closely linked to foraging performance.

Optimal photoreceptor wavelength positions were determined for each of these habitats by using the criterion of maximal color distances between all floral color loci as above (Fig. 7). The results are consistent for all the six habitats: the optimal photoreceptors always occur at those wavelengths where they are positioned in trichromatic bees, at around 340, 430 and 540 nm. For the flowers that bloom under a closed forest canopy, such as those from the German continental forest, the illuminant may deviate substantially from normfunction D65 (Fig.1). Thus, the same model calculation is performed using a forest shade illumination function from Endler (1993). While the shapes of the curves become flatter, implying that under such conditions the wavelength positions are somewhat less critical, the optimal positions are maintained at similar values: λmax = 330, 430 and 560 nm.

Optimal sets of three color receptor types were also modeled by shifting all three photoreceptors independently, using 20 nm steps (Chittka & Menzel, 1992). All three types were moved from 300–660 nm, so that $\lambda\max(M) > \lambda\max(S)$ and $\lambda\max(L) > \lambda\max(M)$. This variation thus generates 969 sets of photoreceptors. These cover combinations with constant wavelength spacing as in real sets of insect photoreceptors ($\sim$100 nm), but shifted positioning of the entire set. A combination of photoreceptors close to that of primate trichromats is also included (λmax = $\sim$ 440,

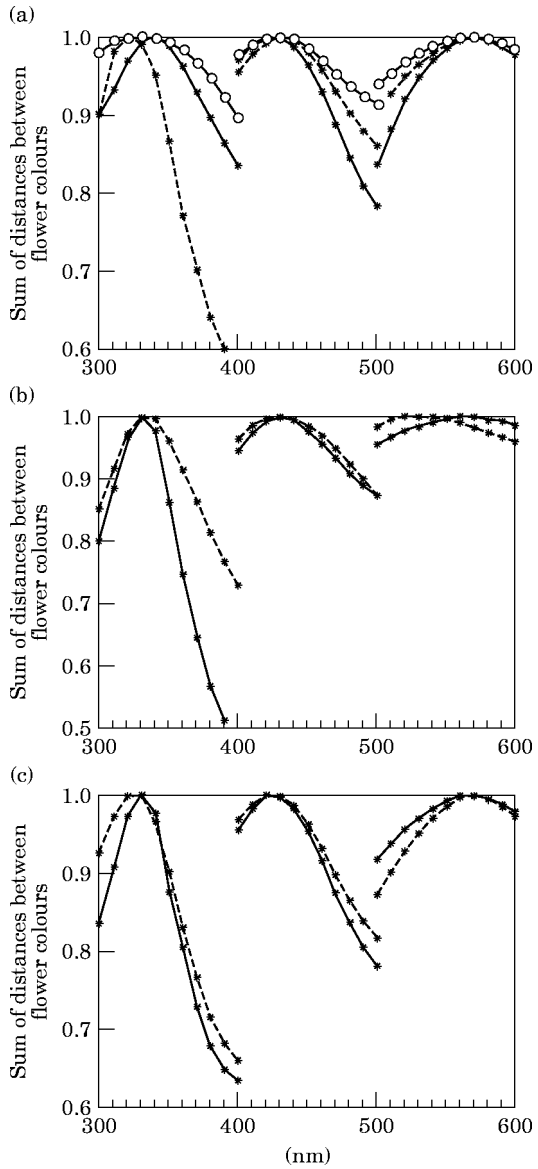

FIG. 7. Optimal color receptors for six sets of sympatric and simultaneously flowering species. As in Figs 5 and 6, the *S* receptor was varied while the *M* and *L* receptors were held constant, then the optimal *M* receptor was determined with the other two fixed, and so forth. (a) —, Israeli desert (25); – –, Continental forest (13); –○–○–○–, Forest illumination. (b) —, Dry grassland (35); – – –, Brazilian cerrado (31). (c) —, Austrian alpine (27); – – –, Norwegian alpine (43). The Israeli data are taken from Menzel & Shmida (1993), the other from (Chittka, 1993; Chittka *et al*., 1994). All flowers are assumed to be illuminated by light following normfunction D65, except those from the German continental forest, for which the same calculations were additionally performed using a forest shade function (Fig. 1, Endler, 1993). Values behind geographical specifications denote the number of species tested.

520 and 560 nm).The quality of the photoreceptor sets produced in this variation was assessed as above, by summing all distances between all color loci. Almost invariably, sets with $\lambda\text{max} = 320$, 420, 560 nm are better than all other combinations tested (Table 1). The small differences between habitats can probably be explained by slightly different distributions of floral color loci, although the frequencies in the six color categories in the hexagon (Chittka *et al*., 1994) are surprisingly similar between most habitats so far tested (Chittka, 1993).

OPTIMAL SETS OF COLOR RECEPTORS AND OPPONENT PROCESSES FOR OBJECT DISCRIMINATION

The environment of a photoreceptor consists not only of the outside world, but also of the brain which it provides with information. The initial stage of color information processing in the bee and wasp visual system is color opponent coding (Chittka *et al*., 1992). It is possible that the optimal color receptors may change when the color opponent system is changed, and vice versa. This is likely since the distribution of color loci in color space changes drastically when the color opponent processes are altered (Fig. 8). So far, we have used a standardized color opponent space, the color hexagon, for our considerations. We will now examine if the optimal receptor wavelength positions will be maintained when subsequent color coding is altered. The same set of 180 Israeli flower colors is used as above.

Figure 9 shows that, indeed, the optimal receptor wavelength positions do depend on the set of opponent processes used. The differences for the optimal *S* receptor are marginal, although the curve shapes differ somewhat from one color opponent system to another. The same is essentially true for the *M* and *L* receptor, where in most cases the optima continue to agree well with the λmax values of Hymenopteran trichromats. However, both for the *M* and *L* receptor, there is one case of opponent system where the curve becomes rather flat in the long wave range and actually has two optima. This concerns the case in which one of the color opponent mechanisms is an *M-S* mechanism without any contribution from the *L* receptor (symbolized by open circles). Thus, while in most cases so far tested the optimal color receptors are independent of the opponent coding system, there may be exceptions to this rule.

We will now examine this question further, by (a) generating a large range of color opponent systems; and (b) calculating, for each of these systems, the optimal λmax values for three spectral photoreceptors by varying all three receptors independently along the wavelength scale. Three opponent mechanisms are considered [see eqns (12–14)]: *S* vs. *ML* (eqn 12), *M* vs. *SL* (13), and *L* vs. *SM* (14), and each of them with weighting factors varied in five steps (see Methods). These mechanisms will be combined in pairs 12 & 13, 12 & 14 and 13 & 14, to form

TABLE 1
The optimal wavelength positions of S, M and L-receptors for several sets of natural colors

	λmax *S*	λmax *M*	λmax *L*	Illuminant
Norwegian alpine	320	420	560	D65
Austrian alpine	320	420	560	D65
Continental forest	320	420	560	D65
Continental forest	340	440	580	Forest shade
Dry grassland	320	420	560	D65
Cerrado	340	420	560	D65
Desert	340	420	560	D65
Green foliage	320	420	560	D65
Green foliage	320	440	580	Forest shade
Fruits	320	520	580	D65

All three receptors are varied independently in 20 nm steps over the range from 300 to 660 nm.

two-dimensional color opponent systems. For each of these combinations, there are 25 (5×5) possibilities with specific weighting factors.

In Fig. 10, three matrices are shown which correspond to these three combinations, with 5×5 possibilities each, corresponding to the specific combinations of weighting factors. The λmax of the optimal color receptors are quite insensitive to the particular color opponent system used. For a wide range of such systems the optimal color receptors are placed at 320 nm for the *S*-receptor, 420–440 nm for the *M*-receptor, and 540–560 nm for the *L*-receptor, which matches well with the three types of color receptors found in 40 species of Hymenoptera (Peitsch *et al*., 1992). Only for a single combination of two color opponent mechanisms do we find a trichromatic set in which the deviation of one of the optimal λmax from those of real Hymenoptera exceeds 20 nm (right matrix, 5th row, 4th column, where λmax $L = 580$ nm). In a few cases of color opponent systems, the model calculations find an optimal solution where two of the λmax are identical, i.e. the optimal receptor set then consists of only two photoreceptors.

Which systems are these? Figure 10 shows that dichromacy is favored precisely in those color opponent systems which revert to the one-dimensional condition, i.e. where the angles between the color hexagon axes are small, as in lower right corner of the right and the lower matrix, and the upper right corner of the left matrix. The shaded area of Fig. 11 can be compared with the shaded areas in Chittka *et al*. (1992, fig. 8), which show the range of color opponent systems that can account for behavioral color discrimination data in nine species of bees and wasps. The shaded areas are clearly similar in shape. The implication is that, with the sets of two color opponent processes possibly implemented in Hymenoptera, the optimal photoreceptor wavelength positions will remain stable and independent of the precise weighting factors of the opponent system.

When one searches for the best possible color opponent system by comparing the total sums of color distances between all flowers (values in brackets in each square), one finds that this optimum is located in the corners marked by thick black arrows, i.e. for a combination of one UV vs. blue mechanism and a UV vs. green mechanism. The distribution of floral color loci in a color space whose metrics are determined by these two mechanisms is shown in Fig. 8 (middle). However, the precise combination of color opponent mechanisms can hardly be considered critical, since the total sums of color differences do not differ substantially between squares. The minimum of 9347 (lower matrix, third row, fourth column) is only 20% below the maximum at 11 695.

Differences in quality of various color opponent systems become much more pronounced when another optimization criterion is used. Figure 11 shows the optimal photoreceptor wavelength positions for the same range of color opponent systems as Fig. 10, but in this case only the three nearest-neighbor-distances are calculated from each flower color locus (see above). With this criterion, the optimal receptor wavelength positions for each color opponent system are even more stable than when all distances between color loci are taken into account. Almost invariably, the optimal λmax are 320, 420–440 and 540–560 nm. In no cases do the calculations arrive at an optimum where two photoreceptors have identical wavelength positions as in Fig.10. There are, however, a few combinations of color opponent mechanisms where $\lambda\max(M) = 400$ nm, which differs from the most frequent *M* receptors in bees by 30 nm. What is noticeably different in comparison with Fig. 10 is the degree to which different color opponent systems produce different total sums of color distances between floral

color loci. The maximum sum of color distances is 16.5 (squares shaded dark gray) whereas the minimal sum reaches only 24% of this value, 3.9. This minimum occurs in dichromatic cases, where two identical opponent mechanisms both combine the inputs from the same two receptor types (lower right corner in the right and lower matrix, and the upper left corner in the upper left matrix).

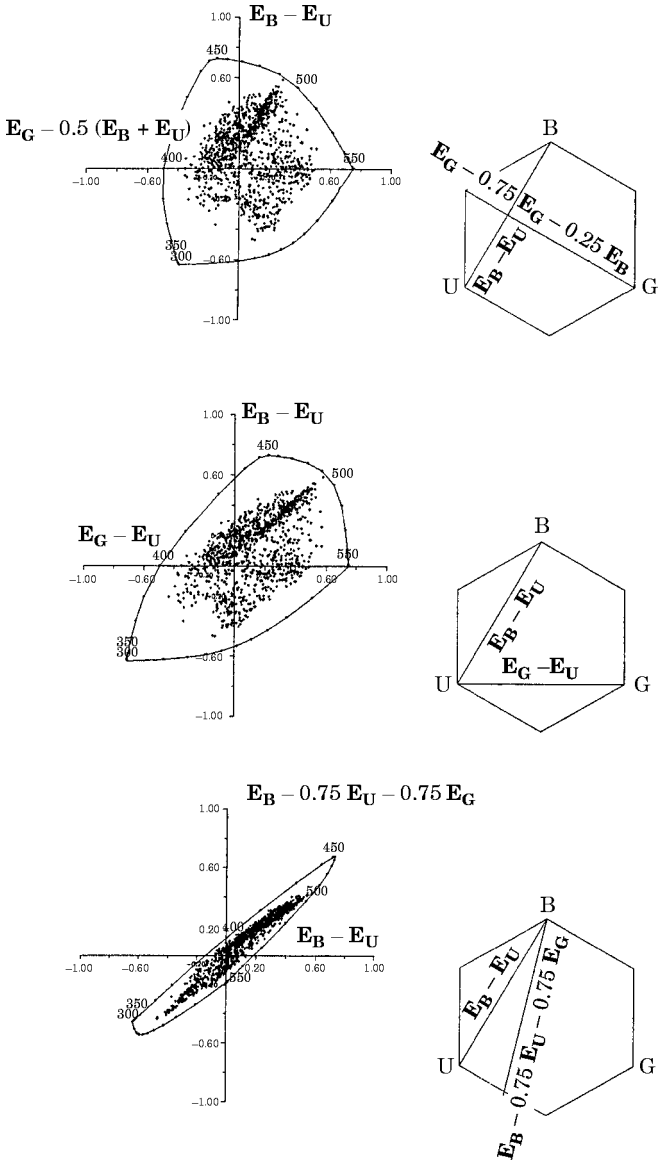

FIG. 8. The spread of color loci depends not only on wavelength position of color receptors, but also on opponent coding. This is exemplified using three combinations of two color opponent mechanisms. The same set of flower color loci is displayed as in Fig. 4. Mechanisms are specified both with weighting factors and by giving their angular orientation in the color hexagon. One of the two mechanisms is a B-U mechanism in all three systems; the other is varied. The spectrum locus is calculated for background light intensity from 300 to 550 nm. For further explanation see Fig. 4.

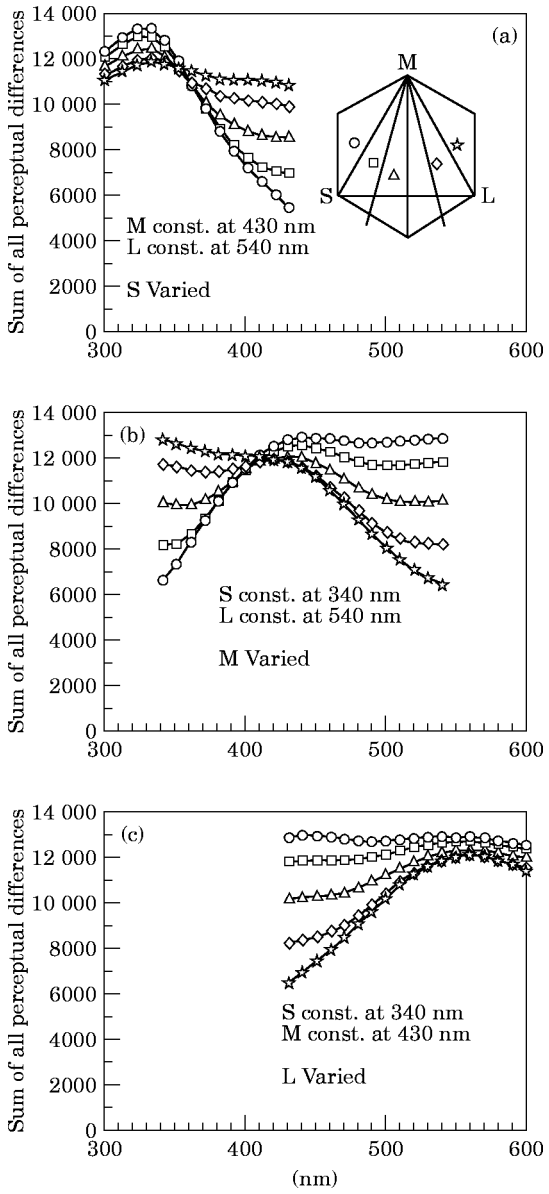

FIG. 9. Optimal color receptors for five different color opponent systems. Two receptors were clamped constant in the three variations, and the third was varied over the indicated range. This procedure was repeated five times for five different combinations of color opponent processes. In all of them, one of the processes is an *L*-*S* mechanism as indicated by the horizontal axis in the inset. The second axis is an $M - (aS + cL)$ mechanism, where $a + c = 1$ and a is varied in five steps from 0 to 1, as shown by the five axis through the hexagon inset. The curves in the three subfigures link symbols which correspond to one particular color opponent axis as indicated by the symbols in the inset. The ordinate specifies the total sum of all distances between floral color loci.

As in Fig. 10, the maximal sum of color distances is found for a combination of an *S* vs. *L* opponent mechanism and an *S* vs. *M* mechanism. However, there are several combinations of other mechanisms which yield sums of color differences only marginally below this value. Seven

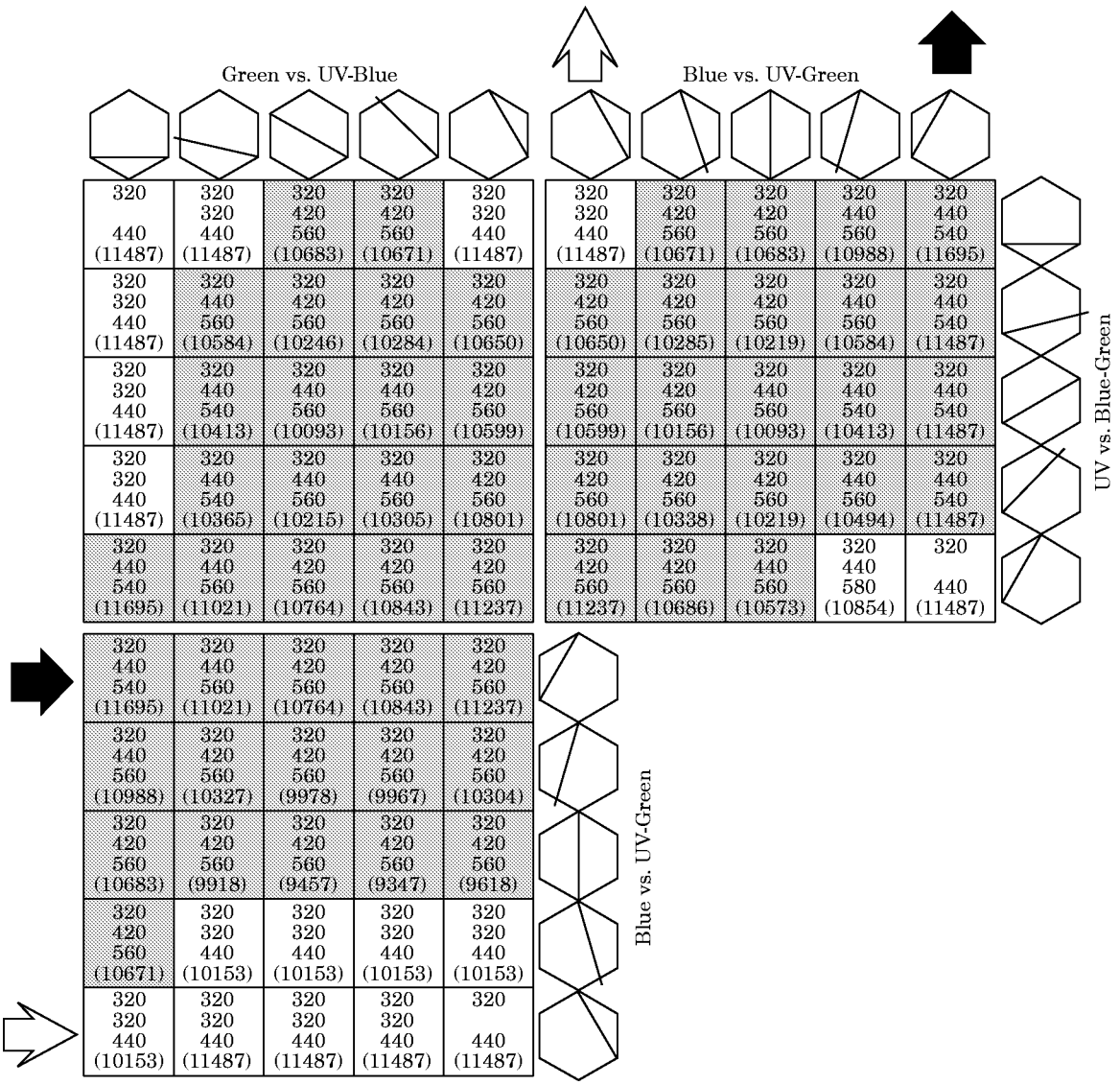

320 440 (11487)	320 320 440 (11487)	320 420 560 (10683)	320 420 560 (10671)	320 320 440 (11487)
320 320 440 (11487)	320 440 560 (10584)	320 420 560 (10246)	320 420 560 (10284)	320 420 560 (10650)
320 320 440 (11487)	320 440 540 (10413)	320 440 560 (10093)	320 440 560 (10156)	320 420 560 (10599)
320 320 440 (11487)	320 440 540 (10365)	320 440 560 (10215)	320 440 560 (10305)	320 420 560 (10801)
320 440 540 (11695)	320 440 560 (11021)	320 420 560 (10764)	320 420 560 (10843)	320 420 560 (11237)

320 320 440 (11487)	320 320 440 (11487)	320 420 560 (10683)	320 420 560 (10671)	320 320 440 (11487)
320 420 420 560 (10650)	320 420 420 560 (10285)	320 420 420 560 (10219)	320 440 560 (10584)	320 440 540 (11487)
320 420 420 560 (10599)	320 420 560 (10156)	320 440 560 (10093)	320 440 560 (10413)	320 440 540 (11487)
320 420 420 560 (10801)	320 420 560 (10338)	320 420 560 (10219)	320 440 560 (10494)	320 440 540 (11487)
320 420 440 560 (11237)	320 420 560 (10686)	320 420 560 (10573)	320 440 580 (10854)	320 440 (11487)

320 440 540 (11695)	320 440 560 (11021)	320 420 560 (10764)	320 420 560 (10843)	320 420 560 (11237)
320 440 560 (10988)	320 420 560 (10327)	320 420 560 (9978)	320 420 560 (9967)	320 420 560 (10304)
320 420 560 (10683)	320 420 560 (9918)	320 420 560 (9457)	320 420 560 (9347)	320 420 560 (9618)
320 420 560 (10671)	320 320 440 (10153)	320 320 440 (10153)	320 320 440 (10153)	320 320 440 (10153)
320 320 440 (10153)	320 320 440 (11487)	320 320 440 (11487)	320 320 440 (11487)	320 440 (11487)

FIG. 10. The range of color opponent systems for which the optimal color receptors are close to those of trichromatic bees. Three matrices are shown which specify the combinations of opponent mechanisms modeled. Each square in the matrices is assigned to one particular combination of two color opponent mechanisms. The specific weighting factors for each square are denoted by color hexagon symbols in the margin of the matrix. The matrices are connected because each shares common rows or columns with the two others. Where this connection cannot be made directly, by placing the matrices next to each other, this is indicated by arrows. Each color hexagon symbol contains one axis which specifies the weighting factors for a given color opponent mechanism [see Chittka (1992) for details]. For each combination of two color opponent mechanisms, the optimal color receptors are determined by varying all three color receptors freely along the wavelength scale from 300 to 660 nm in 20 nm steps, with the only restriction that $\lambda_{max}(L) > \lambda_{max}(M)$ and $\lambda_{max}(M) > \lambda_{max}(S)$. Thus, 969 sets of color receptors are generated for each color opponent system. The λmax of the respective optimal color receptors for each model are given in each square; the value in brackets below denotes the total sum of color distances between all flower colors for that particular color opponent system with the color receptors shown above. The shaded area marks the range of color opponent models for which none of the three color receptors have λmax with >20 nm difference to the most frequent λmax in trichromatic Hymenoptera (i.e. 340, 430, 540 nm; Peitsch *et al*., 1992).

models of 61 tested are only 1% worse than the optimum. More than a third (22) of all models lie in the area shaded light gray, which comprises all systems with color discriminability up to 10% below the optimum.

OPTIMAL COLOR RECEPTORS FOR NON-FLORAL OBJECTS

Finally, optimal wavelength positions are determined for the discrimination of two sets of non-floral objects, using the "nearest-neighbor optimality

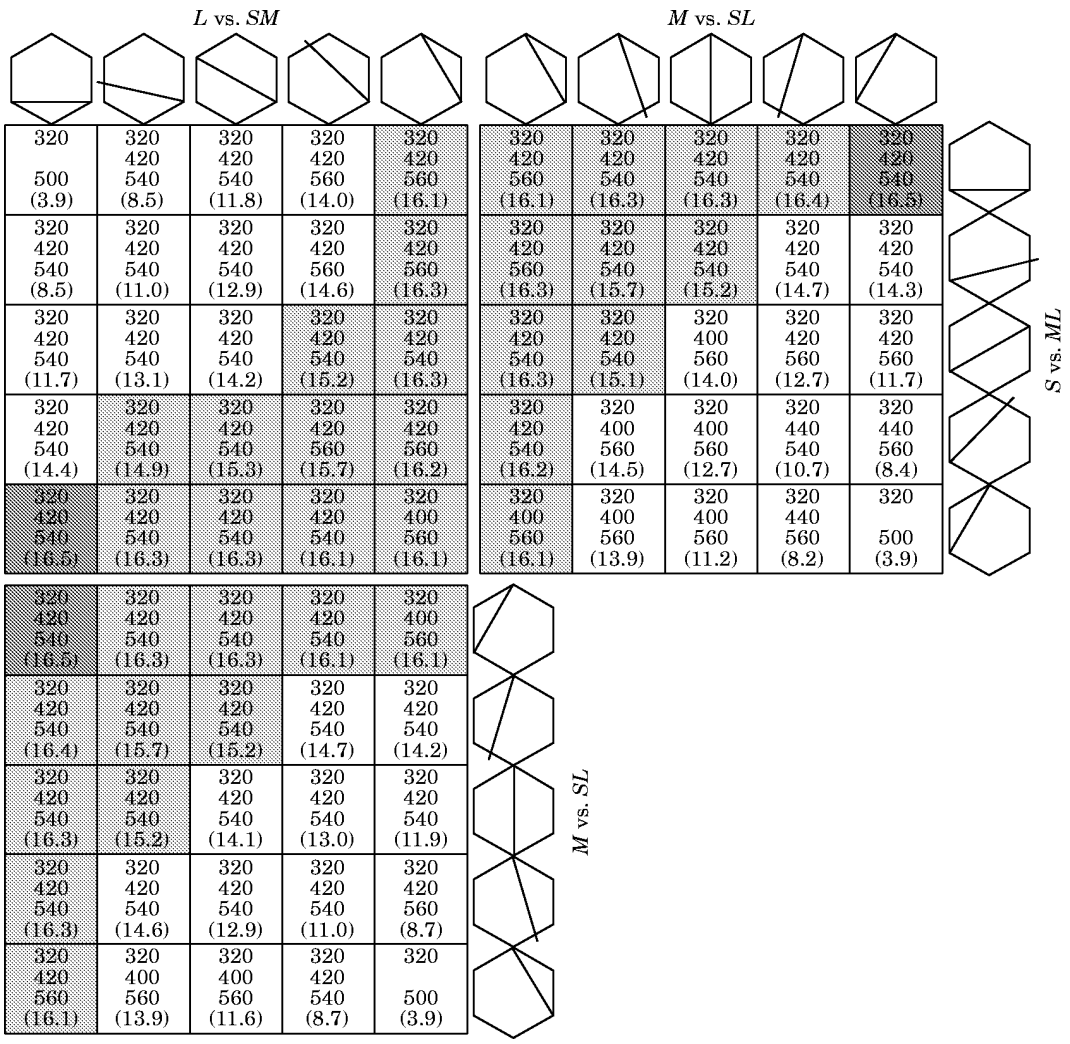

320 500 (3.9)	320 420 540 (8.5)	320 420 540 (11.8)	320 420 560 (14.0)	320 420 560 (16.1)
320 420 540 (8.5)	320 420 540 (11.0)	320 420 540 (12.9)	320 420 560 (14.6)	320 420 560 (16.3)
320 420 540 (11.7)	320 420 540 (13.1)	320 420 540 (14.2)	320 420 540 (15.2)	320 420 540 (16.3)
320 420 540 (14.4)	320 420 540 (14.9)	320 420 540 (15.3)	320 420 560 (15.7)	320 420 560 (16.2)
320 420 540 (16.5)	320 420 540 (16.3)	320 420 540 (16.3)	320 420 540 (16.1)	320 400 560 (16.1)

320 420 560 (16.1)	320 420 540 (16.3)	320 420 540 (16.3)	320 420 540 (16.3)	320 420 540 (16.4)
320 420 560 (16.3)	320 420 540 (15.7)	320 420 540 (15.2)	320 420 540 (14.7)	320 420 540 (14.3)
320 420 540 (16.3)	320 420 540 (15.1)	320 400 560 (14.0)	320 420 560 (12.7)	320 420 560 (11.7)
320 420 540 (16.2)	320 400 560 (14.5)	320 400 560 (12.7)	320 440 540 (10.7)	320 440 560 (8.4)
320 400 560 (16.1)	320 400 560 (13.9)	320 400 560 (11.2)	320 440 560 (8.2)	320 500 (3.9)

320 420 540 (16.5)	320 420 540 (16.3)	320 420 540 (16.3)	320 420 540 (16.1)	320 400 560 (16.1)
320 420 540 (16.4)	320 420 540 (15.7)	320 420 540 (15.2)	320 420 540 (14.7)	320 420 540 (14.2)
320 420 540 (16.3)	320 420 540 (15.2)	320 420 540 (14.1)	320 420 540 (13.0)	320 420 540 (11.9)
320 420 540 (16.3)	320 420 540 (14.6)	320 420 540 (12.9)	320 420 540 (11.0)	320 420 560 (8.7)
320 420 560 (16.1)	320 400 560 (13.9)	320 400 560 (11.6)	320 420 540 (8.7)	320 500 (3.9)

FIG. 11. Optimal receptor wavelength positions for the same range of color opponent systems as in Fig. 9. Values in brackets show the sum of all sets of three nearest-neighbor-distances from all flower colors. The dark gray area marks the combination of color opponent mechanisms with the highest such sum. The area shaded light gray encompasses all color opponent systems which generate a sum of color distances maximally 10% below the optimum. For further explanations see Fig. 10.

criterion". For distinguishing the shades of green foliage, the same set of color receptors is optimal as for flower colors. Depending on whether an insect is flying within forest shade or open space, different wavelength positions of photoreceptors might be optimal. However, the best possible sets of photoreceptors are independent of whether the normfunction D65 or the forest shade function (Endler, 1993) is used as illuminant. For the sample of fruits employed here, only the *S* receptor variation has an optimum comparable to that yielded by flower and leaf colors. The *M* receptor position has little effect on the spread of these fruit colors in color space, and the effectiveness of the *L* receptor increases monotonously towards longer wavelengths (Fig. 12). For the set of leaf colors, I then increased the number of independently varied photoreceptors, in a similar

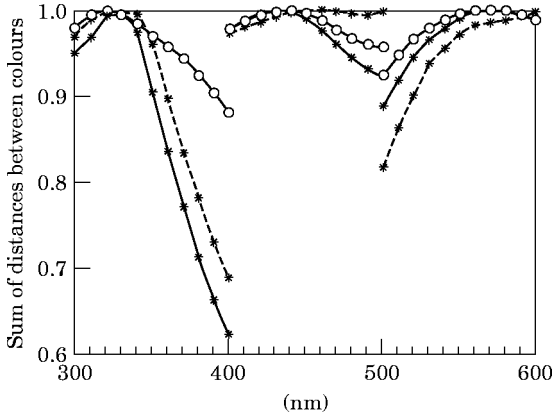

FIG. 12. Optimal sets of color receptors for discrimination of leaves and fruits. For green foliage, the procedure is repeated for two illumination functions (D65 and forest shade) whereas for fruits, only D65 is employed. See Figs 5–7 for more explanation. Key: —, leaves (230); – – –, fruits (35), ⊖ ⊖ ⊖, leaves, forest illuminated.

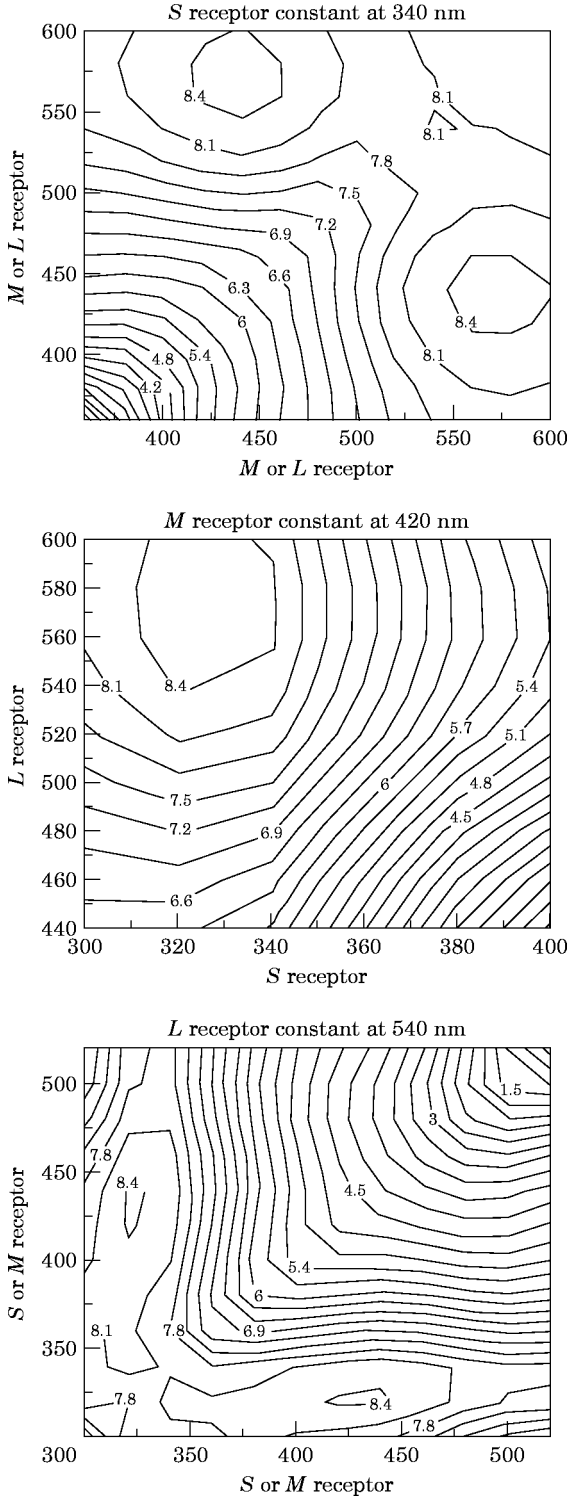

FIG. 13. Optimal pairs of photoreceptors for discrimination of green leaves. In each of three variations, one receptor is constant at the wavelength value where it most frequently occurs in Hymenoptera. The other two are varied in 20 nm steps as denoted by the scale values. Topographical lines mark the sum of all nearest neighbor distances between leaf loci. From each point, the three nearest neighbors are taken into account. D65 is used as the illumination function.

way as was done to determine optimal photoreceptor wavelength positions for flower color coding (Chittka & Menzel, 1992). In each of three model calculations, one receptor was kept constant at a wavelength position where it most frequently occurs in Hymenoptera. The other two are varied in 20 nm steps over a large wavelength range (Fig. 13). In the first model calculation, the *S* receptor was clamped at 340 nm, while the two others were varied from 360 to 600 nm. The optimum for the *M* and *L* receptors occurs at around 440 nm and 560–580 nm. When the *M* receptor is in a fixed position at 420 nm, the optimal *S* receptor is found near 320 nm, while the optimal *L* receptor should be at >540 nm. In the third model calculation, the *L* receptor is held constant at 540 nm, and the other two are varied between 300 and 520 nm. The optimal *M* receptor, then, is found at 420–440 nm and the optimal *S* receptor at 320 nm (Fig. 13).

Finally, optimal sets of three photoreceptors were generated by shifting all photoreceptors independently along the wavelength scale. While the results for various types of green foliage are similar to those for flowers, the set of fruit colors requires an optimal set of color receptors that does not exist in nature (Table 1).

Discussion

The observation that bee color vision is close to optimal for coding of flower colors (Chittka & Menzel, 1992; Chittka *et al*., 1993) is further substantiated here, using several sets of flower colors, as well as novel criteria for optimality. These include the maximization of nearest neighbor differences between color loci and the optimization of the distance between floral color loci and green foliage. Moreover, it is demonstrated that the optimal color receptors are largely independent of the particular color opponent system used to evaluate the receptor signals.

OPTIMAL SPACING OF PHOTORECEPTORS

When only a single receptor wavelength position is varied, and the two others kept at constant wavelengths, the result tells us mostly *how far* the varied photoreceptor should be from the others on the wavelength scale, not necessarily what its absolute best position is under conditions when all three receptors are variable. In other words, it might be possible to shift all three receptors in concert, while keeping the spacing constant, and produce a color vision system with the same quality. But the spacing of photoreceptors, in itself, is a critical aspect of color

vision, and so it will be discussed separately in this section.

When plotted over a wavelength scale, photoreceptors have a roughly Gaussian sensitivity with a halfband width of about 100 nm (e.g. Menzel & Backhaus, 1991). According to Shannon & Weaver (1963), sampling units with Gaussian properties should have peak sensitivities separated by a value that corresponds to their halfband width. This condition is well met by photoreceptor sets of most insects (Menzel & Backhaus, 1991), as well as the modeled results presented here. However, when coding of natural objects with broad reflectance functions is concerned, it is not quite so obvious why this should be the case. If reflectance functions were randomly distributed, two photoreceptors should provide maximally independent information (and thus, best discrimination performance) when their sensitivities overlap minimally, or not at all. In this sense, it is not surprising that the optimal *M*—receptor is located halfway between fixed *S*- and *L*-receptors. By placing the *M* receptor midways between the two other receptors, overlap with both peripheral receptors is minimized, and the receptor will provide maximally independent information from the two other types. However, for the *S* and *L*-receptors, one might expect performance to increase monotonically as they are shifted further away from the *M* receptor. This is not the case. The informational value in the *L*-receptor decreases, if only slightly, at wavelengths above the optimum of 550–560 nm. The same is found for the *S*-receptors positioned below 330 nm. Reflectance falls off drastically in many UV-reflecting flowers below 340 nm (Chittka *et al*., 1994), and so a shift of the *S*-receptors to shorter wavelengths may not pay off. It is less easy to see why the *L*-receptor should not be shifted to longer wavelengths than 560 nm. Actually, reflectance in most flowers is constant or even increases above 600 nm (Chittka *et al*., 1994). However, the long wavelength reflectance in all but the pure red flowers is invariably coupled with reflectance in other spectral domains (the UV, blue, or green part of the spectrum, Chittka *et al*., 1994) and so moving the *L*-receptor to longer wavelengths might actually decrease its value rather than providing additional information.

In summary, spacing of photoreceptors on the wavelength scale is a trade-off between shifting peak sensitivities as far apart as possible to code for independent information, and making maximal use of the information provided by the spectral characteristics of a given class of objects. In nature, this trade-off appears to produce a result which can be predicted by the model calculations presented here.

OPTIMAL WAVELENGTH POSITIONS OF THREE PHOTORECEPTOR TYPES

When all three photoreceptors are shifted along the wavelength scale independently, the model calculations find similar optima as when only single receptors are varied. This indicates that not only the spacing, but also the absolute positions of three photoreceptors types are critical for color coding. The best fit is obtained for the *M*-receptor. In all model calculations, the optimal *M*-receptor lies at 420–430 nm, which corresponds very closely to most insect *M* receptors (Menzel & Backhaus, 1991; Chittka, 1996). Even when only the *M*-receptor is varied, this model calculation is evolutionarily relevant, since early Arthropods might only have had UV and green receptors (Menzel, 1979; Chittka, 1996), and required an adaptive positioning of blue receptors at some point.

In the other two receptors, the fit between optimal and real photoreceptor wavelength positions is not quite as accurate. In several model calculations, the optimal *S* receptors are positioned at somewhat shorter wavelengths (320–330 nm) than the most frequent *S*-receptors in insects ($\sim\lambda\max = 340$–350 nm). Likewise, insect green receptors are consistently found at somewhat shorter wavelengths ($\sim\lambda\max = 540$ nm) than the optimal ones produced by the models (550–560 nm). The reasons for this discrepancy are elusive. Certainly there is no intensity limitation in that range of the spectrum, as might be the case for the short wavelength margin. It has been suggested that the *L*-receptor might be adapted to match green foliage background (Menzel & Backhaus, 1991, Chittka & Menzel, 1992). However, green leaves reflect maximally at 550 nm, which is likewise longer than the maximal sensitivity in most insect green receptors. Thus, it is hard to see why, over several 100 million years of insect evolution, the *L* receptors have not been matched more perfectly to green foliage, if background matching is at all a fitness-limiting task (see also Goldsmith, 1990). Nevertheless, the deviations between optimal and actual photoreceptor wavelength positions appear small when one considers the wide range of models that were generated. Moreover, the positions of real bees' *S* and *L* receptors (at around 340 and 540 nm) yield discriminability of natural objects which is only slightly below that of the optimal positions ($<5\%$ in all cases).

WHAT IS THE BEST POSSIBLE OPPONENT SYSTEM?

The search for a set of two color opponent processes which maximize the discriminability of

floral colors provides less unambiguous results. For determination of such a system, I used a strategy which was already adopted for tackling the color opponent systems most likely to underlie color discrimination of several species of Hymenoptera (Chittka *et al*., 1992). That is, instead of determining only a single best model, a whole range of different models is generated, and their effectiveness in coding color (or in explaining color choices in the 1992 study) is compared. This method is advantageous because it allows us to judge whether a given model is truly better than other, similar models, or whether the difference is insignificant.

Opponent systems with orthogonal axes, by definition, should contain the highest amount of information. However, since the color loci are unevenly dispersed in a general color space such as the hexagon, it is necessary to test whether there is any set of two color opponent axes that optimizes the spread of color loci in such a way that discrimination of all stimuli will be favored. In case there is no such specific system, it is interesting to see if the algorithm will select as best all those color opponent systems whose axes are orthogonal in the hexagon.

With both optimality criteria [maximizing (1) all color distances or (2) only those of nearest neighbors], the best possible color opponent system for discriminating a set of 180 flower colors consists of one UV vs. blue and one UV vs. green mechanism. However, this pair of opponent mechanisms cannot be considered substantially better than a whole range of other such pairs. The different color opponent models generated in this study are simply linear transformations of one another. Thus, they will produce sets of color distances that will often differ only marginally from one system to another (Chittka *et al*., 1992). In this sense it is hardly surprising that there is no single combination of color opponent mechanisms that is significantly better than all others for distinguishing a given set of objects. The quality of a color opponent system for this task can be assessed by measuring the degree of orthogonality of color opponent axes in the hexagon, rather than the precise weighting factors of the single opponent processes (Chittka, 1992).

Does the range of color opponent systems generating large color distances between natural colors in Fig. 11 comprise combinations of color opponent mechanisms whose assigned axes make large angles in the hexagon? Yes. The shaded area in Fig. 11 (which includes the best possible models and those which generate color discriminability up to 10% below this optimum) includes only models with color opponent axes whose angles are 60° or larger. Thus, for the task of maximizing color differences between extremely similar flower colors, it is critical to possess two color opponent mechanisms which differ strongly in their weighting factors, and, correspondingly, whose axes differ substantially in terms of their orientation in the hexagon.

Finally, it is interesting to compare the color opponent models that flower visitors should have for theoretical purposes with those models that best explain behavioral color discrimination data in Hymenopterous insects. To this end, Fig. 11 can be matched with Fig. 7 in Chittka *et al*. (1992). In that figure, the shaded areas mark those models that are most likely to account for color discrimination in the respective insects, whereas Fig. 11 shows models which code natural colors most efficiently. In both figures, these areas are noticeably similar in shape; they only comprise models whose color opponent axes have large angles in the hexagon. Hence, color opponent coding in trichromatic bees and wasps is well suited for the task of maximizing distinctiveness of flower colors.

WAS BEE COLOR VISION EVOLUTIONARILY TUNED TO CODE FLOWER COLORS?

Bee color vision is close to optimal for coding flower colors on several distinct levels. Since detection and discrimination of floral colors are of vital interest for obligatory flower visitors such as many species of bee, selection will certainly stabilize bee color vision with its current traits. Any series of mutation events generating a color vision system whose components differ from the optima determined in this study will impair foraging success, and consequently, fitness. But do these results mean that bee color vision was evolutionarily tuned to discriminate between flower colors in the first place? The general problem with evolutionary optimization procedures of the kind described here is that one can only disprove a hypothesis conclusively, not confirm it. In other words, had the optimal photoreceptors as derived from the model calculations been radically *different* from the ones found in "real animals", this would have been sound evidence that evolution has *not* optimized the photoreceptors according to the same criteria. At the very least it would mean that there are other, more important criteria, or that evolutionary constraints might have hindered the animal from evolutionarily proceeding along the same lines as the model calculations. The fact that the calculations arrive at similar color vision systems as nature is tempting, but it does *not* necessarily imply that one has found the criterion which has driven the evolution of bee color vision. There might be other criteria that

are equally or more important for the respective organism (and which arrive or have earlier arrived at the same optimal solution) or the photoreceptors found in Hymenoptera might simply be an effect of evolutionary constraints (Goldsmith, 1990), and just happen to be optimal for an arbitrarily picked task.

In fact, sets of color receptors similar to those of bees occur in animals which occupy entirely different ecological niches, such as the beach isopod *Ligia* (Hariyama *et al*., 1993) the backswimmer *Notonecta* (Bruckmoser, 1968), nocturnal hawkmoths (White *et al*., 1994), and the larval ocelli of some Lepidoptera (Ichikawa & Tateda, 1982). This indicates that Arthropod color receptor positions actually predate the evolution of flower color. The observation that bee color vision is optimally suited to code flower color can probably be explained when one assumes that flower colors adapted to insect vision, and that, as a consequence, they contain the information about the receiver to which they were addressed.

Even though the wavelength positions of insect UV, blue and green receptors appear to be evolutionarily inert, it is inconceivable that sensitivity of these receptors has been maintained for a very long time without stabilizing selection. As few as three amino acid substitutions can cause a shift of 30 nm in peak spectral sensitivity (Neitz *et al*., 1991), and so the evolutionary stability of the respective visual pigments is likely to have an adaptive explanation. Since phylogenetic analyses show that bee color vision is probably older than flowers (Chittka, 1996), we must look for visual tasks relevant to animals in a pre-angiosperm world.

One such task is the discrimination of green leaves. Lythgoe & Partridge (1989) have determined the optimal set of two visual pigments for this task, and found that the best solution is a receptor at $\lambda\max = 420$–450 nm in combination with a second receptor maximally sensitive at 480–560 nm. Here, an optimal third receptor is determined as well. The optimal M and L receptors found here ($\lambda\max(M) = 420$–460 nm; $-\lambda\max(L) = 540$–580 nm) are in good agreement with the two types found by Lythgoe & Partridge (1989), although the short wavelength end of the range of the optimal L receptor occurs at noticeably longer wavelengths in the present study. The optimal third receptor is located at $\lambda\max = 320$ nm in all model calculations. Thus, the best possible photoreceptor set for leaf discrimination is also in good agreement with those normally found in trichromatic Hymenoptera, with the same deviations as when flower discrimination is concerned. This raises the possibility that sets of UV–blue–green receptors constitute an ancient adaptation which is optimal for several classes of natural objects, so long as these are not specifically adapted to a different visual system, as are fruits. Further model calculations with other classes of natural objects, such as sand and stones, are necessary to test this possibility.

I wish to thank Drs R. Menzel and M. Vorobyev for stimulating discussions in the early phase of this work, and Dr J. Endler for the forest shade illumination spectrum in Fig. 1. The helpful criticism of the two anonymous referees is gratefully appreciated.

REFERENCES

Abramov, I. & Gordon, J. (1994). Color appearance: On seeing red—or yellow, or green, or blue. *Annu. Rev. Psychol.* **45**, 451–485.

Backhaus, W. (1991). Color opponent coding in the visual system of the honeybee. *Vision Res.* **31**, 1381–1397.

Backhaus, W. (1992). The Bezold-Brücke effect in the color vision system of the honeybee. *Vision Res.* **32**, 1425–1431.

Brandt, R., Backhaus, W., Dittrich, M. & Menzel, R. (1993). Simulation of threshold spectral sensitivity according to the color theory for the honeybee. In: *Gene—Brain—Behaviour. Proceedings of the 21st Göttingen Neurobiology Conference* (Elsner, N. & Heisenberg, M., eds), p. 374. Stuttgart: Georg Thieme Verlag.

Bruckmoser, P. (1968). Die spektrale Empfindlichkeit einzelner Sehzellen des Rückenschwimmers *Notonecta glauca L.* (Heteroptera). *Z. vergl. Physiol.* **59**, 187–204.

Chittka, L. (1992). The color hexagon: a chromaticity diagram based on photoreceptor excitations as a generalized representation of colour opponency. *J. Comp. Physiol.* [*A*] **170**, 533–543.

Chittka, L. (1993). The colour perception of hymenoptera, the colours of flowers, and their evolutionary and ecological relationship. PhD thesis, FU Berlin.

Chittka, L. (1996). Does bee colour vision predate the evolution of flower colour? *Naturwissenschaften* **83**, 136–138.

Chittka, L., Beier, W., Hertel, H., Steinmann, E. & Menzel, R. (1992). Opponent colour coding is a universal strategy to evaluate the photoreceptor inputs in hymentoptera. *J. Comp. Physiol.* [*A*] **170**, 545–563.

Chittka, L. & Menzel, R. (1992). The Evolutionary Adaptation of Flower Colors and the Insect Pollinators' Color Vision Systems. *J. Comp. Physiol.* [*A*] **171**, 171–181.

Chittka, L., Vorobyev, M., Shmida, A. & Menzel, R. (1993). Bee colour vision—the optimal system for the discrimination of flower colours with three spectral photoreceptor types? In: *Sensory Systems of Arthropods* (Wiese, K., Gribakin F.G., Popov, A. V. & Renninger, G., eds), pp. 211–218. Basel/Switzerland: Birkhäuser Verlag.

Chittka, L., Shmida, A., Troje, N. & Menzel, R. (1994). Ultraviolet as a component of flower reflections, and the colour perception of hymenoptera. *Vision Res.* **34**, 1489–1508.

Daumer, K. (1958). Blumenfarben wie sie die Bienen sehen. *Z. vergl. Physiol.* **41**, 49–110.

Dittrich, M. (1995). A quantitative model of successive color induction in the honeybee. *J. Comp. Physiol. A* **177**, 219–234.

Endler, J. A. (1992). Signals, signal conditions, and the direction of evolution. *American Naturalist* **139**, 125–153.

Endler, J. A. (1993). The color of light in forests and its implications. *Ecological Monographs* **63**, 1–27.

Feinsinger, P. (1987). Effects of plant species on each other's pollination: is community structure influenced? *TREE* **2**, 123–126.

Giurfa, M., Nunez, J., Chittka, L. & Menzel, R. (1995). Colour choice of flower-naive honeybees. *J. Comp. Physiol. A* **177**, 247–259.

Goldsmith, T. H. (1990). Optimization, constraint, and history in the evolution of eyes. *Quart. Rev. Biol.* **65**, 281–322.

Hariyama, T., Tsukuhara, Y. & Meyer-Rochow, V. B. (1993). Spectral responses, including a UV-sensitive cell type, in the eye of the isopod Ligia exotica. *Naturwissenschaften* **80**, 233–235.
Helversen, O.v. (1972). Zur spektralen Unterschiedsempfindlichkeit der Honigbiene. *J. Comp. Physiol.* **80**, 439–472.
Ichikawa, T. & Tateda, H. (1982). Distribution of Color Receptors in the Larval Eyes of Four Species of Lepidoptera. *J. Comp. Physiol.* **149**, 317–324.
Jacobs, G. H. (1993). The distribution and nature of colour vision among the mammals. *Biol. Rev.* **68**, 413–471.
Kevan, P. G. & Baker, H. G. (1983). Insects as flower visitors and pollinators. *Annu. Rev. Entomol.* **28**, 407–453.
Laughlin, S. B. (1989). The role of sensory adaptation in the retina. *J. Exp. Biol.* **146**, 39–62.
Lipetz, L. E. (1971). The Relation of Physiological and Psychological Aspects of Sensory Intensity. In: *Handbook of Sensory Physiology* (Loewenstein, W. R., ed.), pp. 192–225. Berlin: Springer.
Lythgoe, J. N. (1979). *The Ecology of Vision*. Oxford: Clarendon Press.
Lythgoe, J. N. & Partridge, J. C. (1989). Visual pigments and the acquisition of visual information. *J. Exp. Biol.* **146**, 1–20.
Lythgoe, J. N. & Partridge, J. C. (1991). The modelling of optimal visual pigments of dichromatic teleosts in green coastal waters. *Vision Res.* **31**, 361–371.
Menzel, R. (1979). Spectral sensitivity and colour vision in invertebrates. In: *Invertebrate photoreceptors* (*Handbook of Sensory Physiology*, *Vol.VII*/6*A*) (Autrum, H., ed.), pp. 503–580. Berlin: Springer.
Menzel, R. & Backhaus, W. (1991). Colour Vision in Insects. In: *Vision and Visual Dysfunction*. *The Perception of Colour* (Gouras, P., ed.), pp. 262–288. London: Macmillan Press.
Menzel, R. & Shmida, A. (1993). The ecology of flower colours and the natural colour vision of insect pollinators: The Israeli flora as a study case. *Biol. Rev.* **68**, 81–120.
Nagle, M. G. & Osorio, D. (1993). The tuning of human photopigments may minimize red-green chromatic signals in natural conditions. *Proc. R. Soc. Lond. B* **252**, 209–213.
Naka, K. I. & Rushton, W. A. H. (1966). S-potentials from colour units in the retina of fish (Cyprinidae). *J. Physiol.* **185**, 536–555.
Neitz, M., Neitz, J. & Jacobs, G. H. (1991). Spectral Tuning of Pigments Underlying Red-Green Color Vision. *Science* **252**, 971–974.
Peitsch, D., Fietz, A., Hertel, H., de Souza, J., Ventura, D. F. & Menzel, R. (1992). The spectral input systems of hymenopteran insects and their receptor-based colour vision. *J. Comp. Physiol.* [*A*] **170**, 23–40.
Shannon, C. E. & Weaver, W. (1963). *The Mathematical Theory of Communication,* Urbana; University of Illinois Press.
Stavenga, D. G., Smits, R. P. & Hoenders, B. J. (1993). Simple exponential functions describing the absorbance bands of visual pigment spectra. *Vision Res.* **33**, 1011–1017.
Valberg, A., Seim, T., Lee, B. B. & Tryti, J. (1986). Reconstruction of equidistant color space from responses of visual neurones in macaques. *J. Opt. Soc. Am. A* **3**, 1726–1734.
Waser, N. M., Chittka, L., Price, M. V., Williams, N. & Ollerton, J. (1996). Generalization in pollination systems, and why it matters. *Ecology* **77,** 1043–1060.
White, R. H., Stevenson, R. D., Bennett, R. R. & Cutler, D. E. (1994). Wavelength discrimination and the role of ultraviolet vision in the feeding behavior of hawkmoths. *Biotropica* **26**, 427–435.
Wyszecki, G. & Stiles, W. S. (1982). Color Science, Concepts and Methods, Quantitative Data and Formulae, New York: Wiley.